Optics Communications 98 (1993) 357–365
North-Holland

OPTICS
COMMUNICATIONS

Full length article

Mechanism of photorefractive enhancement of photochromic gratings in BSO – experimental results and phenomenological modelling

P.M. Jeffrey, S.L. Clapham, R.W. Eason
Department of Physics and Optoelectronics Research Centre, University of Southampton, Southampton, SO9 5NH, UK

D.A. Fish, A.K. Powell, T.J. Hall
Department of Physics, King's College, Strand, London, WC2R 2LS, UK

and

N.A. Vainos
FO.R.T.H.–I.E.S.L, P.O. Box 1527, Heraklion 711 10, Crete, Greece

Received 7 September 1992

We report an increase of more than a factor of 100 in the diffraction efficiency from photochromic gratings written in BSO, by uniformly illuminating these gratings with 488 nm light to induce secondary photorefractive gratings. Upon application of an electric field, the phase shift between the two gratings can be varied and under appropriate conditions the diffraction efficiency can increase. The dependence of the enhanced diffraction efficiency as a function of the applied electric field and readout beam polarisation was experimentally investigated for two different crystal orientations. Phenomenological modelling is presented requiring modifications to the phase angle between the photochromic and induced photorefractive gratings in order to reproduce the experimentally observed asymmetry in the increase in the diffraction efficiency. This suggests a periodic modulation of the photorefractive donor/acceptor density, due to the presence of the photochromic grating.

1. Introduction

$Bi_{12}SiO_{20}$ (BSO) is a photorefractive crystal which has found numerous applications in two beam coupling (2BC) and four-wave mixing (FWM) experiments [1]. Two standard crystal orientations are used for such holographic experiments, the first with the grating wavevector $K_G \| \langle 001 \rangle$ (standard configuration for two beam coupling as shown in fig. 1a) and the second with the grating vector $K_G \perp \langle 001 \rangle$ (standard configuration for four-wave mixing as shown in fig. 1b). Permanent discoloration of crystals such as BSO and other related sillenite crystals such as BGO and BTO, has been observed during crystal growth and high power laser experiments. This was initially referred to as optical damage and thought to be undesirable, since these photochromic regions exhibited increased absorption, reducing the intensity of any beams involved in photorefractive processes.

Writing photochromic gratings in photorefractive materials such as BSO [2–4] however, offers the possibility of permanent information storage due to the characteristics of these photochromic gratings. Photochromic gratings have very long dark storage times (more than three years so far in our experiments), and once information has been written in these crystals it is essentially permanent at room temperature, assuming non destructive readout. If however, the photochromic region of the crystal is continually exposed to high power laser illumination of an appropriate wavelength, then the fringe visi-

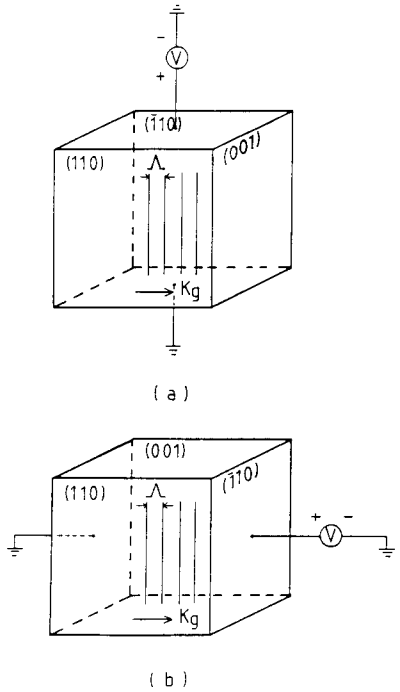

Fig. 1. Two experimental BSO crystal configurations used for these experiments. (a) $K_G \| \langle 001 \rangle$ orientation for maximum energy exchange. (b) $K_G \perp \langle 001 \rangle$ orientation for maximum diffraction efficiency.

bility of the photochromic gratings will be lost. At room temperature these photochromic effects in BSO are essentially irreversible, but it is possible to remove the areas of photochromic discoloration by heating the crystal in silicone oil at 200 °C for a period of one hour. Applications involving multiplexed photochromic and photorefractive gratings [3] are of interest because of the possibility of multiplexing two essentially distinct holographic gratings, which do not have to be recorded at the same time, or with the same laser. The separate natures of the photochromic and induced photorefractive gratings, allows simple phenomological modelling of the combined effects, which we present in this paper along with experimental results.

Applications involving multiplexed photochromic and photorefractive gratings are numerous and extend to retrieval systems and other interferometric applications [5]. Photorefractive gratings offer the possibility of dynamic information storage and retrieval where the relatively fast response time of BSO, as compared with other photorefractive crystals such as $BaTiO_3$, allows operation at speeds comparable to TV frame rates. The low diffraction efficiencies obtainable with BSO (typically $\leqslant 0.1\%$) is a disadvantage for possible future applications in planar waveguides and communication systems, and techniques of controllably enhancing the diffraction efficiency seem to be very important if industrial applications are to be realised.

The results that we present in this paper combine the two very different photochromic and photorefractive mechanisms of BSO, offering a very versatile storage medium allowing both temporary and permanent information to be stored, with controllable diffraction efficiency. We show that the diffraction efficiency is dependent principally upon the crystal orientation used, the applied electric field and the polarisation of the readout beam.

The technique of photoconductively enhancing the crystal to produce large increases in the diffraction efficiency is a simple technique which does not require large intensities. Diffraction efficiency which is controllable simply by rotating the polarisation of the readout beam or altering the applied electric field is a desirable feature for optical switching, coupling and interconnections and is potentially applicable to fibre optic communications.

2. Experimental configuration

Photochromic gratings were written in a 10 mm × 10 mm × 2 mm BSO crystal mounted with electrodes on the $\langle \bar{1}10 \rangle$ face and orientated for maximum diffraction efficiency as shown in fig. 1b. The experimental configuration is shown in fig. 2, showing the set up for writing the photochromic gratings (beams 1 and 2 – Ar^+ at 488 nm) and enhancing the gratings (beam 5 – Ar^+ at 488 nm) and measuring the diffraction efficiency of the combined photochromic and induced photorefractive gratings with a readout beam (beams 3 and 4 – HeNe at 633 nm). The writing beams used to initially write the photochromic gratings were vertically polarised with $I_1 = I_2 = 50$ mW, and a full writing angle $2\theta = 25°$ (corresponding to a fringe spacing of $\Lambda = 1.13$ μm).

Under conditions of suitable temperature stability, photochromic gratings were written within a pe-

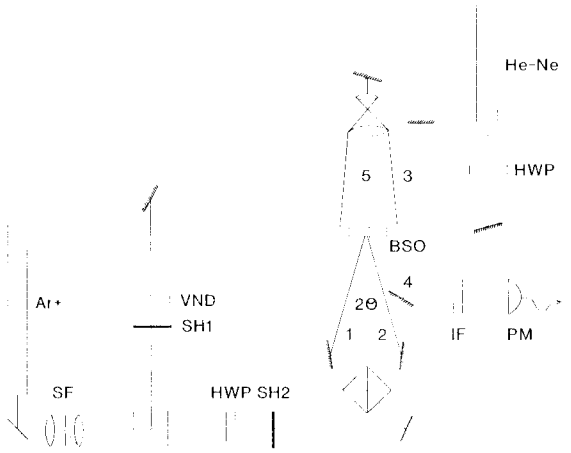

Fig. 2. Experimental setup used to write photochromic gratings in BSO. IF = 633 nm interference filter; HWP = half wave plate; PM = power meter; SH = shutter; VND = variable neutral density filter.

riod of 20–30 minutes. If writing of the photochromic gratings was continued for a longer period of time, then the diffraction efficiency of the gratings monitored by the Bragg matched readout beam, was observed to saturate after 40–60 minutes, and if prolonged exposure was continued then the diffraction efficiency was observed to decrease.

A 633 nm HeNe interference filter in front of the calibrated power meter (Newport model 835) filtered out any stray light at 488 nm, allowing only the weak HeNe diffracted readout beam to be measured. The measured diffraction efficiencies without the presence of the enhancing beam were characteristically low with a 3 mW beam incident on the rear of the 2 mm thick BSO crystal producing a maximum diffraction intensity of 0.920 μW (0.03% without compensating for absorption and mirror loses) and a maximum photochromic diffraction intensity of 0.330 μW (just over one third of the maximum joint primary photorefractive and photochromic diffraction intensity, showing that the grating strength of the primary photorefractive grating was approximately double that of the photochromic grating).

Once the photochromic gratings had been written in the BSO, the writing beams were then permanently blocked using shutter SH2. Shutter SH1 was used to control the expanded enhancing beam (488 nm) which homogeneously illuminated the crystal. The enhancing beam ($I_5 = 7.5$ mW) was incident normally upon the rear of the BSO crystal to ensure uniform illumination.

3. Experimental results

Figure 3a shows how the enhancement factor was experimentally observed to vary as a function of the applied electric field for the $K_G \perp \langle 001 \rangle$ configuration. The enhancement factor was defined to be the ratio of the intensity of the diffracted HeNe readout beam with the blue enhancing beam illuminating the photochromic grating, to that of the intensity of the diffracted beam without the presence of the blue enhancing beam. Results for the $K_G \parallel \langle 001 \rangle$ configu-

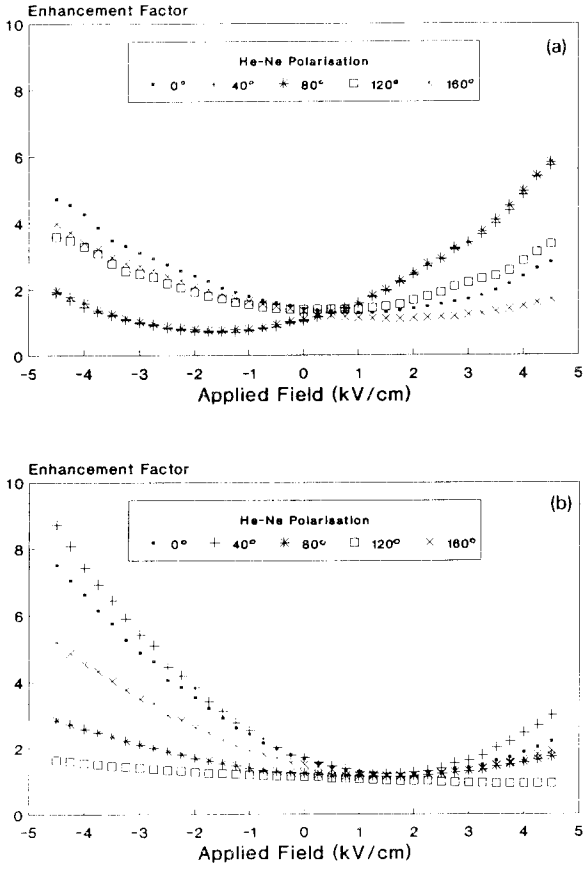

Fig. 3. Experimental results of enhancement factor as a function of applied field for different polarisation of readout beam for two different crystal configurations: (a) $K_G \perp \langle 001 \rangle$, (b) $K_G \parallel \langle 001 \rangle$.

ration are shown in fig. 3b. The angle of the HeNe polarisation was defined to be that with respect to the vertical axis, where all angles represent clockwise rotations with respect to the forward direction of the beam.

As is seen in fig. 3a, it was observed in all experiments that there was a point of convergence for the $K_G \perp \langle 001 \rangle$ orientation around 0.5 kV cm^{-1} and for the $K_G \parallel \langle 001 \rangle$ orientation around 1.5 kV cm^{-1}. For the $K_G \parallel \langle 001 \rangle$ configuration the maximum enhancement effects were seen for increasing negative applied fields. The maximum enhancement factor of 9.33 was observed for a readout beam polarisation of 20° and an applied field of -4.5 kV cm^{-1}. For a readout polarisation of 110° the enhancement factor was observed to be effectively independent of the applied field, staying constant at around 1.5. For the $K_G \perp \langle 001 \rangle$ configuration the maximum enhancement factor was observed either for negative or positive applied fields depending upon the readout beam polarisation. A relatively lower maximum enhancement factor of 6.3 was obtained for an applied field of $+4.5$ kV cm^{-1} with a readout beam polarisation of 60°. Asymmetric polarization properties have also recently been reported [6] in BTO where fast and slow holograms have exhibited different polarization properties and erasure characteristics.

The effect of varying the polarisation of the readout beam with positive applied fields is shown in fig. 4a for the $K_G \perp \langle 001 \rangle$ configuration. The maximum enhancement factor obtained increased with increasing applied electric field. For applied fields $> +1$ kV cm^{-1}, maxima were observed at a readout polarisation of 65°, and minima were observed at a polarisation angle of 155°, but the minimum enhancement factor was always greater than unity. For an applied field of $+1$ kV cm^{-1} the enhancement factor was independent of the readout beam polarisation with a value of 1.2. For applied fields $< +1$ kV cm^{-1} the minimum enhancement factor dropped below unity showing de-enhancement, and the enhancement factor was seen to take on a different characteristics as can be seen from fig. 4b, where minima were observed for a readout beam polarisation of 65°. Maximum were observed for a readout beam polarisation of 155° (exactly opposite to the case with applied fields $> +1$ kV cm^{-1}). The maximum enhancement factor for negative applied fields was reduced as compared to positive applied fields.

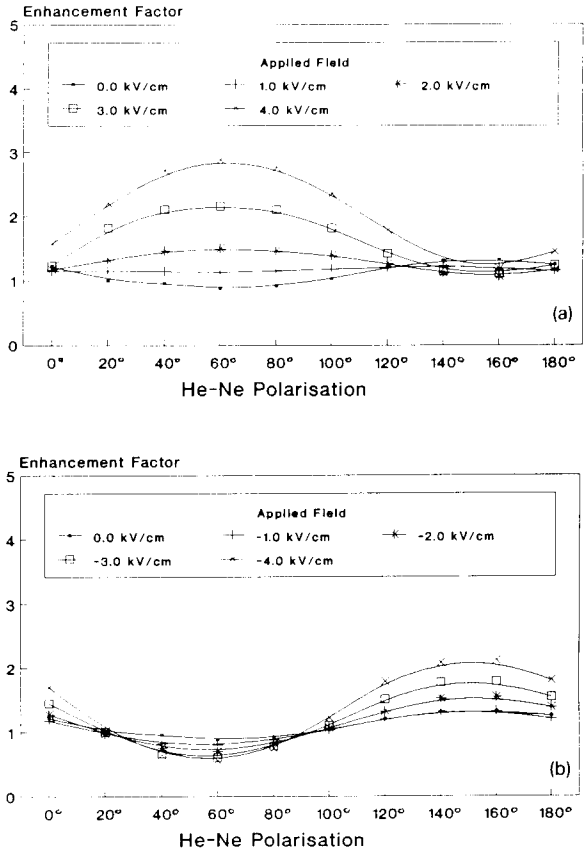

Fig. 4. Experimental results of enhancement factor for the $K_G \perp \langle 001 \rangle$ configuration, as a function of readout beam polarisation for (a) positive applied fields, (b) negative applied fields.

4. Phenomological modelling

A vectorial model was formulated to investigate the asymmetry in the observed results for the enhancement factor, by assuming the increase in the diffraction efficiency to be the sum of the contributions from the permanent photochromic gratings and the secondary induced photorefractive gratings. It was assumed that a permanent photochromic grating recorded in BSO, had an associated modulation of the absorption coefficient of the crystal, which was unshifted with respect to the intensity interference pattern of the two original writing beams. Illumi-

nation of the photochromic grating with a blue enhancing beam induced a secondary photorefractive grating which was ϕ out of phase with respect to the permanent photochromic grating.

The schematic for the enhancement effect is shown in fig. 5. A Bragg matched readout beam encounters two different holographic gratings, so that the diffracted wave is the result of the combined diffraction from both the photochromic and the induced photorefractive grating. The amplitude of the diffracted field E_1, from the photochromic grating, was assumed to be independent of the applied electric field, and did not undergo a phase shift upon reflection from the grating. The amplitude of the diffracted field from the induced photorefractive grating E_2, undergoes a $\psi = \pm\pi/2$ phase shift on reflection, which is positive if the readout beam is Bragg matched from the left hand side and reversed sign if Bragg matched from the opposite direction. In the experiment as shown in fig. 2 the readout beam was Bragg matched from the left hand side ($\psi = +\pi/2$).

The enhancement effects were modelled for the $K_G \perp \langle 001 \rangle$ crystal orientation by representing the diffracted field from the photochromic grating to be a fixed vector E_1 and vectorially adding a second vector E_2, rotated through an angle γ (to include the effect of optical activity and the polarisation of the readout beam [7]), which represented the photorefractive contribution to the diffracted field. The phase shift ϕ of the photorefractive grating with respect to the photochromic grating was dependent upon the applied external electric field, via

$$\phi = \tan^{-1}\left(\frac{E_d}{E_0}\right)\left(1 + \frac{E_d}{E_q} + \frac{E_0^2}{E_d E_q}\right), \qquad (1)$$

where E_0 is the applied electric field (kV cm^{-1}), E_d the diffusion electric field (kV cm^{-1}), E_q the saturation electric field (kV cm^{-1}).

The total resultant phase shift between light scattered from the two gratings is therefore $(\phi + \psi)$ as shown in fig. 6a. The amplitude of the photorefractive contribution to the diffracted field E_2, is also dependent upon the applied electric field and was calculated using the expression for the efficiency of a thick transmission phase grating [8] recorded in BSO:

$$E_2^2 = \exp\left(\frac{-2\alpha d}{\cos\theta_0}\right)\sin^2\left(\frac{\pi \Delta n d}{\lambda \cos\theta_0}\right), \qquad (2)$$

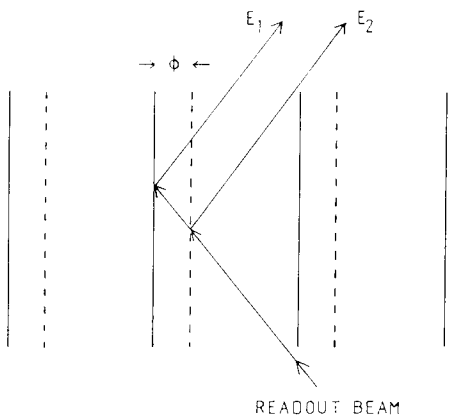

Fig. 5. Schematic used for modelling of enhancement effect, showing the secondary induced photorefractive grating shifted from the permanent photochromic grating by a variable phase angle ϕ.

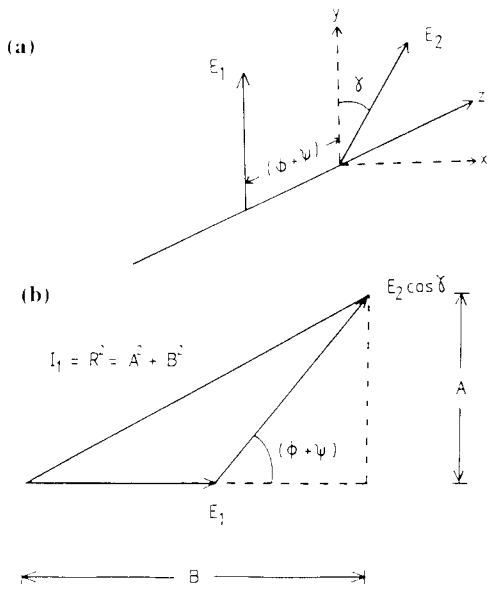

Fig. 6. (a) Diagram depicting the two contributions of diffraction – a contribution due to the photochromic grating E_1 and a second contribution due to the induced photorefractive grating E_2. (b) Vector diagram used to calculate the resultant diffraction intensity from the two gratings.

where Δn is the steady state refractive index modulation, d the thickness of crystal, α the absorption coefficient, θ_0 the Bragg angle, and λ the HeNe wavelength.

The steady state refractive index modulation is given in terms of the space charge field E_{sc}:

$$\Delta n = -\tfrac{1}{2} r_{eff} n_0^3 E_{sc} , \tag{3}$$

$$E_{sc} = m E_q \left(\frac{E_0^2 + E_d^2}{E_0^2 + (E_d + E_q)^2} \right)^{1/2} , \tag{4}$$

where m is the modulation index and r_{eff} the effective electro-optic coefficient.

The electric field dependence of E_2 is derived by substituting equations (3) and (4) into (2):

$$E_2^2 = \exp\left(\frac{-2\alpha d}{\cos\theta_0} \right) \sin^2 \left[\frac{-\pi r_{eff} n_0^3 d m E_q}{2\lambda \cos\theta_0} \times \left(\frac{E_0^2 + E_d^2}{E_0^2 + (E_d + E_q)^2} \right)^{1/2} \right] . \tag{5}$$

In order to model these effects it was necessary to calculate the diffusion and saturation fields. The diffusion field E_d was calculated to be 1.4 kV cm^{-1} from

$$E_d = k_B T K_G / e , \tag{6}$$

where k is Boltzmann's constant, T the temperature, K_G the grating wavevector and e the electronic charge.

The saturation field E_q was calculated to be 7.9 kV cm^{-1}, assuming a representative literature value of $N_A = 1.36 \times 10^{22}$ m^{-3} [9]:

$$E_q = e N_A \Lambda / 2\pi\epsilon\epsilon_0 , \tag{7}$$

where e is the electronic charge, N_A the density of acceptor sites, Λ the fringe spacing and ϵ the relative permittivity.

To evaluate the total diffracted intensity, it was necessary to resolve the components of the photorefractive diffracted field with amplitude E_2, into the directions parallel to, and perpendicular to the photochromic diffracted field with amplitude E_1. In the direction parallel to E_1:

$$E_{2\parallel} = E_2 \cos\gamma \tag{8}$$

and in the direction perpendicular to E_1:

$$E_{2\perp} = E_2 \sin\gamma . \tag{9}$$

The sum of the contribution of diffraction from the two separate gratings in the direction parallel to E_1 (as shown in figure 6(b)) is given by

$$I_1 = [E_2 \cos\gamma \sin(\phi+\psi)]^2 + [E_1 + E_2 \cos\gamma \cos(\phi+\psi)]^2 . \tag{10}$$

In the direction perpendicular to E_1 there is an additional contribution given by

$$I_2 = (E_2 \sin\gamma)^2 . \tag{11}$$

The total diffracted output intensity is $I_1 + I_2$ and therefore, the enhancement factor EF, is given by the expression

$$\mathrm{EF} = (I_1 + I_2)/E_1^2 . \tag{12}$$

Substituting eqs. (10) and (11) into eq. (12) gives

$$\mathrm{EF} = [E_2 \cos\gamma \sin(\phi+\psi)]^2 + [E_1 + E_2 \cos\gamma \cos(\phi+\psi)]^2 + [E_2 \sin\gamma]^2 / (E_1^2) . \tag{13}$$

Which reduces to

$$\mathrm{EF} = (E_2/E_1)^2 + 1 + 2(E_2/E_1)\cos\gamma \cos(\phi+\psi) . \tag{14}$$

On examination of eq. (14), it is clear that the $\cos(\phi+\psi)$ component will exhibit symmetry about $E_0 = 0$ kV cm^{-1} for an initial choice of $\psi = +\pi/2$. Substituting eq. (1) into eq. (13) for the dependence of the phase angle on the applied electric field, allows the enhancement factor to be calculated as a function of applied electric field. This yielded curves of enhancement factor as a function of applied field for the $K_G \perp \langle 001 \rangle$ orientation which were symmetrical about $E_0 = 0$ kV cm^{-1} and which did not intersect at any point (shown in fig. 7). These symmetrical curves are observed due to the symmetry in the phase angle as a function of applied field as shown in fig. 8. Changing the value of the saturation field E_q or the diffusion field E_d did not cause asymmetry in the enhancement factor to be observed.

It was found that it was necessary to increase the phase angle for increasing negative field in order to reproduce the observed asymmetry. Figure 9a shows the effect of increasing the phase angle for negative applied fields assuming a saturation field E_q of 7.9 kV cm^{-1} and a diffusion field E_d of 1.4 kV cm^{-1}. With these parameter values a common intersection

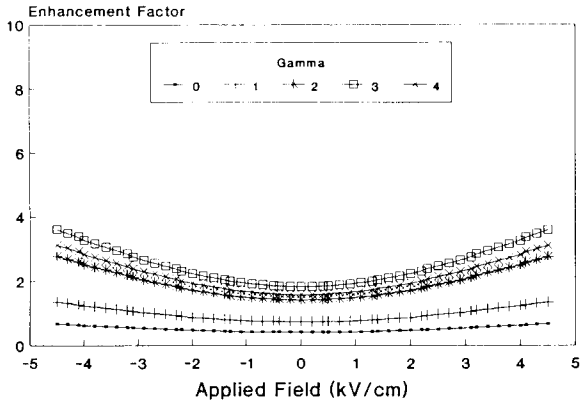

Fig. 7. Theoretical modelling of the enhancement factor as a function of applied field for different values of γ in radians (γ includes the effects of optical activity and rotating the angle of polarisation of the readout beam).

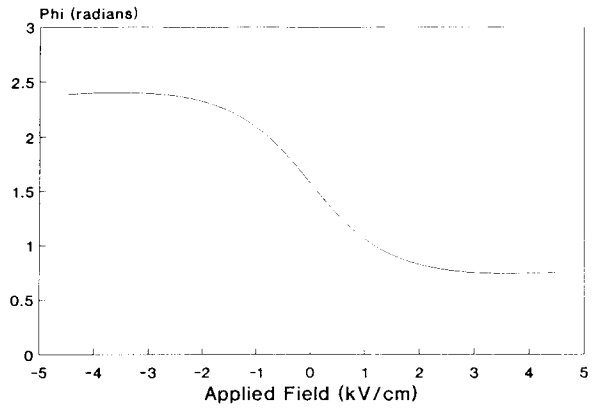

Fig. 8. Variation of phase angle as a function of applied field according to eq. (1). For zero applied field the phase angle $\phi = \pi/2$.

point around 4.5 kV cm^{-1} was observed. If the diffusion field was reduced to 0.14 kV cm^{-1} then the common intersection point was further reduced to 1.1 kV cm^{-1}. These results compare with the experimental results, suggesting that either the calculated diffusion field is too high or that the actual applied field within the photochromic/photorefractive grating interaction region is reduced. The modifications needed to the phase angle may suggest the presence of an in-built field which is revealed upon application of an external electric field or alternatively the presence of a periodically modulated photorefractive donor/acceptor density, due to the presence of the induced photorefractive grating.

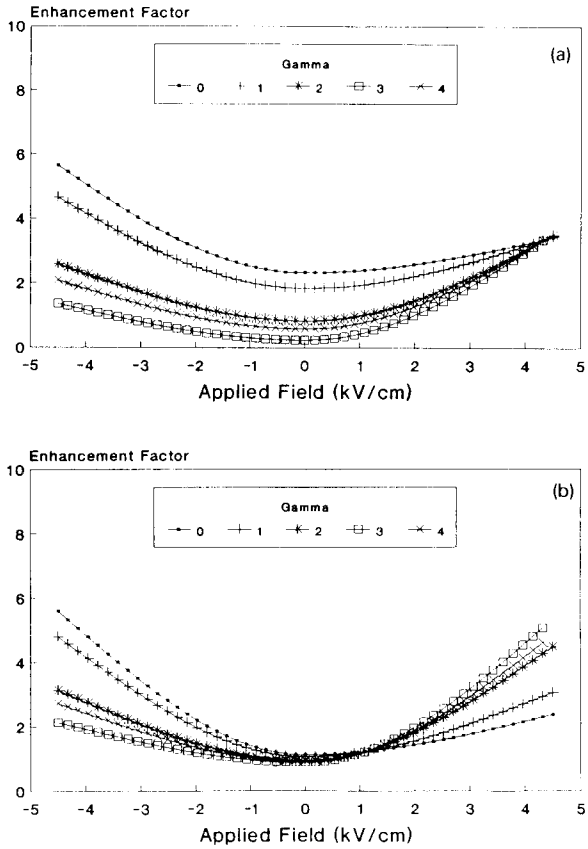

Fig. 9. Theoretical modelling of enhancement factor as a function of applied field for $E_q = 7.9$ kV cm^{-1} and (a) $E_d = 1.4$ kV cm^{-1}, (b) $E_d = 0.14$ kV cm^{-1}.

5. Maximum diffraction efficiency

Experiments were carried out to investigate the conditions under which the largest diffraction efficiency enhancement could be obtained. The technique of photoconductive enhancement [9] uses a second enhancing beam of blue light (488 nm) to strongly increase the conductivity outside the region of the photochromic grating so that most of the applied field is dropped across the combined photochromic and induced photorefractive grating regions. Figure 10 shows the beam geometry required for the technique of photoconductive enhancement.

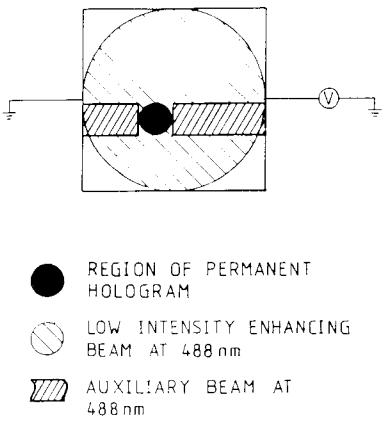

Fig. 10. Technique of photoconductive enhancement using a low intensity enhancing beam and a high intensity auxiliary beam at 488 nm (after ref. [7]).

The effect of the auxiliary blue beam is to strongly increase the conductivity in the regions outside the permanent hologram region, and thus produce very high local fields where essentially all the applied voltage is dropped across the area of interest. With a maximum voltage supply of 6 kV dc, it was therefore possible to produce electric fields of up to 30 kV cm^{-1} across the permanent hologram.

A cylindrical lens was used to produce a narrow rectangular beam of blue light, and with the aid of a mask in front of the crystal, the auxiliary beam was arranged so that it did not overlap the permanent hologram region. A low intensity enhancing beam of 4 mW cm^{-2} was used so that the photochromic gratings were not erased. The HeNe readout beam was linearly polarised at 155° to the vertical, and with maximisation of the intensity (692.5 mW cm^{-2}) and position of the auxiliary blue beam, a maximum enhancement factor of 112 was achieved for an applied voltage of +6.0 kV dc in the $K_G \perp \langle 001 \rangle$ configuration.

Figure 11 shows the experimental curve of the enhancement factor, EF, as a function of an externally applied high electric field, E_0, across a permanent hologram recorded in a crystal of BSO in the $K_G \perp \langle 001 \rangle$ configuration. All experimental parameters were optimised, for this case, in an attempt to establish the maximum enhancement possible. The asymmetry is again evident in the results obtained.

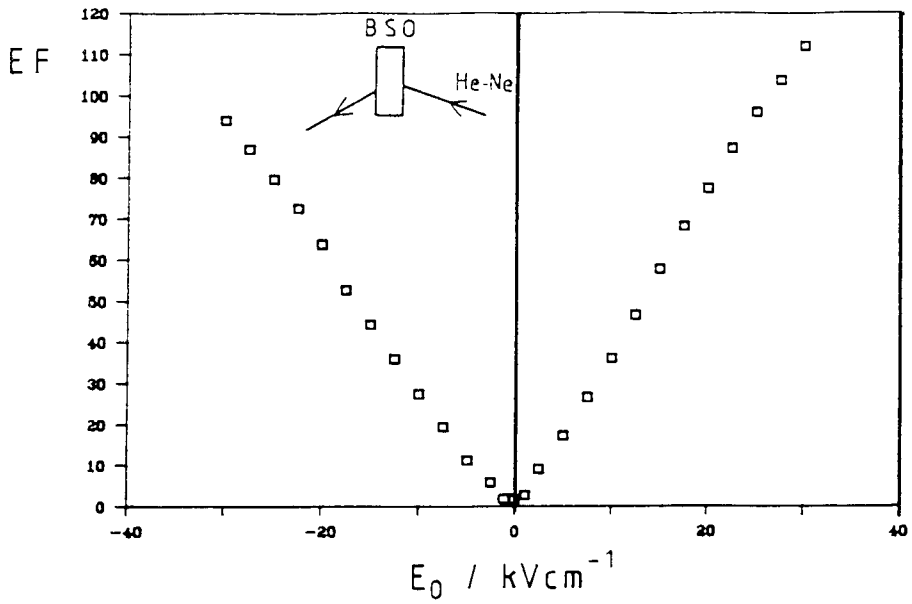

Fig. 11. Experimental curve of the enhancement factor, EF, as a function of an externally applied high electric field, E_0, across a permanent hologram recorded in the $K_G \perp \langle 001 \rangle$ configuration. All experimental parameters have been optimised.

6. Conclusions

In conclusion a maximum enhancement of 112 in the diffraction efficiency of a 633 nm readout beam from a photochromic grating written in BSO, has been obtained by photoconductivity enhancing the crystal with 488 nm light and applying an electric field. The enhancement is due to the presence of an induced secondary photorefractive grating, which was phase shifted from the permanent photochromic grating. In order to successfully model these effects the phase angle between the photochromic grating and the induced photorefractive grating requires modification for high negative applied electric fields. The implementation of these polarisation dependent enhancement effects will be investigated in recently fabricated BSO planar waveguides, and promises potential applications in the areas of optical switching, coupling and interconnects.

Acknowledgements

The authors wish to acknowledge the support of the Science and Engineering Research Council (S.E.R.C.) under grant number GR/F 84256 and GR/H 21531, and for the support of P.M. Jeffrey in the form of a research studentship. This work was performed under the U.K. Phase Conjugation Consortium (POPCON).

References

[1] P. Günter and J.-P. Huignard, Photorefractive materials and their applications II (Springer, Berlin, 1988).
[2] N.A. Vainos, S.L. Clapham and R.W. Eason, Appl. Optics 28 (1989) 4381.
[3] N.A. Vainos, S.L. Clapham and R.W. Eason, Appl. Optics 28 (1989) 4386.
[4] W. Wardzynski, T. Lukasiewicz and J. Zmija, Optics Comm. 30 (1979) 203.
[5] J.P. Huignard, J.P. Herriau and T. Valentin, Appl. Optics 16 (1977) 2796.
[6] A.A. Kamshilin, J. Frejlich and P.M. Garcia, Appl. Optics 31 (1992) 1787.
[7] A. Marrakchi, R.V. Johnson and A.R. Tanguay Jr., J. Opt. Soc. Am. B 3 (1986) 321.
[8] H. Kogelnik, Syst. Tech. J. 48 (1969) 2909.
[9] R.W. Eason and N.A. Vainos, J. Mod. Optics 35 (1988) 491.